Soil Dynamics and Earthquake Engineering 199 (2025) 109668

Contents lists available at ScienceDirect

Soil Dynamics and Earthquake Engineering

journal homepage: www.elsevier.com/locate/soildyn

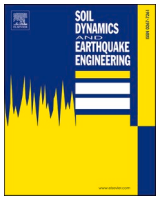

DMT-based liquefaction triggering procedure accounting for the fines content effect

Anna Chiaradonna *, Paola Monaco

Department of Civil, Construction-Architectural and Environmental Engineering, University of L'Aquila, 67100, L'Aquila, Italy

ARTICLE INFO

Keywords:
Flat dilatometer test
Soil liquefaction
Semi-empirical liquefaction chart
Fines content

ABSTRACT

The application of semi-empirical charts based on in-situ testing results represents the first step in the earthquake-induced soil liquefaction assessment. Among them, the CPT-based charts have been largely developed in the last decades, especially after the 2010–2011 Canterbury earthquakes in New Zealand, while the main drawback of the existing approach based on DMT is related to the lack of a correction factor for the fines content. In this regard, this study proposes a new empirical relationship between the cyclic resistance ratio and the horizontal stress index where the effects of the fines content are incorporated. The new method is calibrated on specific sites located in the Emilia-Romagna plain (Italy), where an extensive soil characterization from in-situ and laboratory tests was available for the silty sand and sandy silt deposits affected by liquefaction after the 2012 Emilia earthquake. The performance of the new curve accounting for the fines content effect is compared with that obtained by adopting the "clean sand" curves proposed in the past, as well as with that obtained by using the most recent CPT-based method. Even though verified only for specific Italian soils and requiring further field validation, the proposed approach appears as promising to improve the DMT-based liquefaction assessment in silty sands.

1. Introduction

Simplified methods based on in-situ test results are commonly used for assessment of earthquake-induced soil liquefaction, at least as a first step before performing more complex analyses. In general, the adopted approach lies within the framework of the "simplified procedure" based on the comparison, at any depth, of the seismic demand (cyclic stress ratio *CSR*) and the capacity of the soil to resist liquefaction (cyclic resistance ratio *CRR*). Liquefaction may occur when *CSR* is greater than or equal to *CRR*. The *CSR* is evaluated based on the main characteristics of the assumed scenario earthquake. The *CRR* is commonly estimated by using semi-empirical charts based on the results of in-situ tests, such as the cone penetration test (CPT), the standard penetration test (SPT), shear wave velocity (V_S) measurements, and the flat dilatometer test (DMT). For each in-situ test method, *CRR* is obtained as a function of a normalized and corrected parameter assumed as representative of the soil liquefaction resistance. In the approach implemented by Ref. [1] in CPT- and SPT-based methods, the *CRR* is estimated as a function of a normalized soil resistance parameter, including the effect of the fines content *FC*. The normalized values q_{c1N} (CPT) and $(N_1)_{60}$ (SPT) are converted into equivalent clean sand values q_{c1Ncs} and $(N_1)_{60cs}$, respectively, by introducing the corrections Δq_{c1N} and $\Delta(N_1)_{60}$ depending on *FC*, having the form:

$$q_{c1Ncs} = q_{c1N} + \Delta q_{c1N} \tag{1}$$

$$(N_1)_{60cs} = (N_1)_{60} + \Delta(N_1)_{60} \tag{2}$$

Hence, both q_{c1Ncs} and $(N_1)_{60cs}$ are obtained as the sum of two terms: the first one (q_{c1N}, $(N_1)_{60}$) is related to the normalization of the measured data to the effective overburden stress, the second one (Δq_{c1N}, $\Delta(N_1)_{60}$) accounts for the beneficial effect of the fines content, which is "fictitiously" translated into an increase of the soil resistance parameters (q_{c1Ncs}, $(N_1)_{60cs}$).

In particular, in the CPT-based framework provided by Ref. [1] the following terms are defined in order to obtain the equivalent clean sand cone resistance q_{c1Ncs}:

$$q_{c1N} = C_N \cdot \frac{q_c}{P_a} \tag{3}$$

* Corresponding author.
E-mail address: anna.chiaradonna1@univaq.it (A. Chiaradonna).

https://doi.org/10.1016/j.soildyn.2025.109668
Received 31 December 2024; Received in revised form 10 July 2025; Accepted 14 July 2025
Available online 19 July 2025

$$C_N = \left(\frac{P_a}{\sigma'_v}\right)^m \leq 1.7 \quad (4)$$

$$m = 1.338 - 0.249 \cdot q_{c1Ncs}{}^{0.264} \quad (5)$$

$$\Delta q_{c1N} = \left(11.9 + \frac{q_{c1N}}{14.6}\right) exp\left(1.63 - \frac{9.7}{FC+2} - \left(\frac{15.7}{FC+2}\right)^2\right) \quad (6)$$

where q_c = measured cone resistance, P_a = atmospheric pressure, σ'_v = effective overburden stress, and FC = fines content (i.e., percentage of soil having particles diameter smaller than 0.075 mm), taken into account by Δq_{c1N}. The value of q_{c1Ncs} must be found by trial and error.

The same authors also provided a relationship to estimate FC from the soil behavior type index I_c; after that, the C_{FC} correction factor is calibrated on experimental data:

$$I_C = \frac{FC+137}{80} - C_{FC} \quad (7)$$

The CPT-based empirical relationship proposed by Ref. [1] is the following:

$$CRR_{M=7.5,\sigma'=1} = exp\left(\frac{q_{c1Ncs}}{113} + \left(\frac{q_{c1Ncs}}{1000}\right)^2 - \left(\frac{q_{c1Ncs}}{140}\right)^3 + \left(\frac{q_{c1Ncs}}{137}\right)^4 - 2.8\right) \quad (8)$$

Eq. (8) provides the cyclic resistance ratio of the soil characterized by a given value of q_{c1Ncs} for a reference 7.5 magnitude earthquake and effective overburden stress equal to 1 atm. Further corrections to Eq. (8) are necessary to take into account: (i) the overburden stress, via the correction factor K_σ, and (ii) the actual magnitude of the earthquake, via the Magnitude Scaling Factor (MSF).

In the case of the SPT, the terms for the calculation of the normalized number of blow counts corrected for energy ratio and fines content $(N_1)_{60cs}$ are defined as follows:

$$(N_1)_{60} = C_N \cdot N_{60} \quad (9)$$

$$m = 0.784 - 0.0768 \cdot (N_1)_{60cs}^{0.5} \quad (10)$$

$$\Delta(N_1)_{60} = exp\left(1.63 + \frac{9.7}{FC+0.01} - \left(\frac{15.7}{FC+0.01}\right)^2\right) \quad (11)$$

where N_{60} is the energy-corrected blow count measured during SPT, C_N is the same of Eq. (4) and $\Delta(N_1)_{60}$ accounts for the effect of the fines content. Similar to CPT, the value of $(N_1)_{60cs}$ must be found by trial and error.

In the widely used charts based on CPT, SPT, and V_S, the CRR curve is defined as an empirical boundary separating datapoints related to liquefaction and no-liquefaction cases observed in real earthquakes. However, while the CPT-based charts in particular have been largely developed in the last decades, for the DMT-based methods, the liquefaction case history database is still limited. In addition, one major drawback of the existing approach for DMT is related to the lack of a correction factor for the fines content in the assessment of the DMT-based cyclic strength of soils.

In this regard, based on the preliminary applications reported in Refs. [2,3], this study proposes a DMT-based liquefaction triggering procedure accounting for the fines content effect by combining the efforts made in the previous studies. Additionally, a new relationship for the estimation of the fines content from the results of DMT is derived from previous studies and compared to the existing equations.

After a brief recall of the DMT-based methods proposed in the past, the new DMT-based liquefaction triggering procedure accounting for the fines content effect is presented (section 3). The new procedure is applied to two Italian sites located in the Emilia-Romagna plain, where an extensive soil characterization from in-situ and laboratory tests is available for the silty sand and sandy silt deposits affected by liquefaction after the 2012 Emilia earthquake (section 4). The performances of the new proposed method have been compared with those obtained by adopting the curve for clean sand proposed by Ref. [4] and that obtained using the CPT-based method by Ref. [1] (section 5).

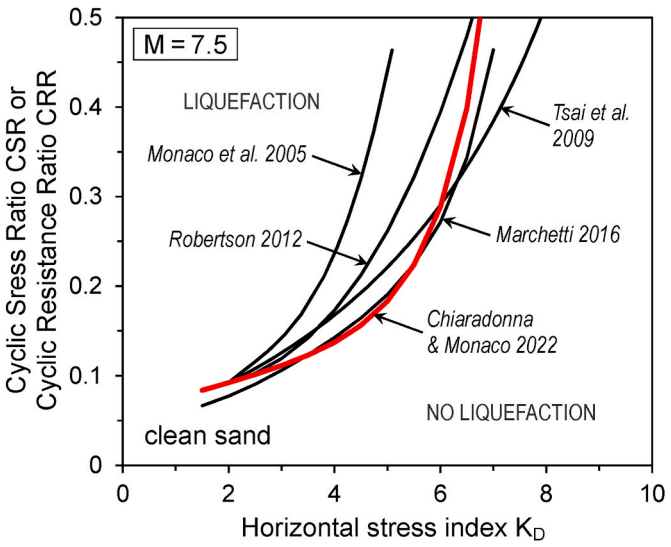

Fig. 1. Summary of recent DMT-based CRR-K_D correlations for clean sands.

2. Background on DMT-based methods for liquefaction assessment

Simplified methods for estimating the CRR based on DMT test results have been proposed over the years. In these methods, the liquefaction triggering curve is defined based on the horizontal stress index K_D, a key parameter obtained from DMT interpretation. The K_D parameter was originally defined by Ref. [5] based on the measured first DMT pressure p_0 normalized to the effective overburden stress. Various studies (e.g., Ref. [6]) have pointed out that K_D reflects cumulatively various stress history effects, i.e., overconsolidation, in-situ stress state, pre-straining/aging, and is correlated with the relative density and the in-situ state parameter. All these factors are known to greatly influence the cyclic strength of soils. Therefore, K_D has been recognized as a suitable index parameter of liquefaction resistance. Hence, K_D can be used in a similar way as the normalized and corrected parameters employed in methods based on other in-situ tests, e.g., the normalized corrected cone tip resistance q_{c1N} for CPT, the normalized

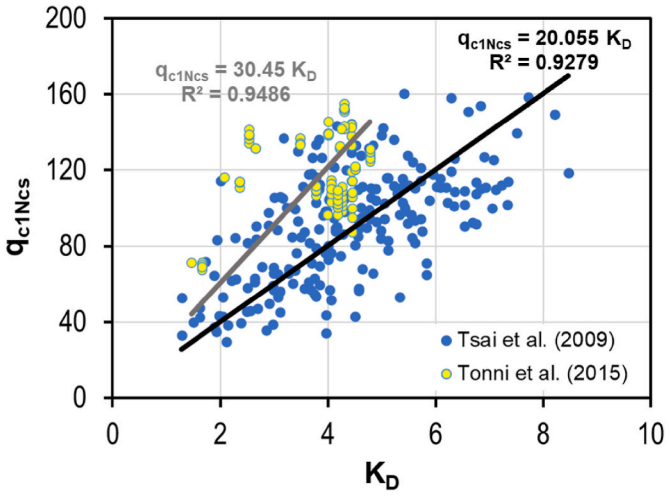

Fig. 2. Relationship between q_{c1Ncs} and K_D from published CPT-DMT data records at different sites [4].

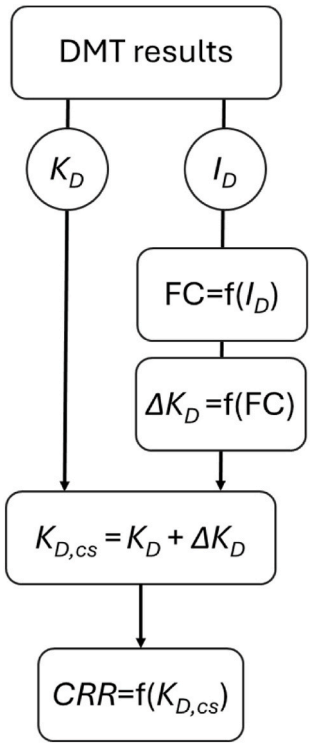

Fig. 3. Scheme of the DMT-based liquefaction triggering procedure accounting for the fines content effect proposed in this study.

energy-corrected blow count $(N_1)_{60}$ for SPT, and the overburden stress corrected shear wave velocity V_{S1}.

Fig. 1 shows a summary of the most recent *CRR*-K_D curves (for magnitude 7.5 earthquakes) proposed by Refs. [6–9], and [4]. The DMT K_D-based methods currently available are valid for clean sand and do not account for the effect of the fines content *FC*.

The field performance database for validation of the DMT-based methods is currently limited. This substantial drawback is partially mitigated by the fact that most DMT-based methods have been formulated by translation of existing liquefaction triggering curves developed for CPT (and SPT), which are instead supported by a vast field performance case history database [10].

Ref. [4], using the CPT-DMT data set by Ref. [7] for five different sites in Taiwan, and considering only CPT data providing a soil behavior type index I_c between 1.5 and 2.6, established a direct correlation between K_D and q_{c1Ncs} (Fig. 2). Despite the dispersion, the Taiwan data set is well described by a linear trend with a slope of 20. Fig. 2 also shows a second data set [11] from the Scortichino site, Italy, where both piezocone (CPTU) and seismic dilatometer (SDMT) data were available, considering only data for $FC < 10$ %. The Scortichino data set is better interpreted by a linear trend with a slope of about 30.

Due to the discrepancy in the two examined datasets, also considering the limited amount of processed data Ref. [4], adopted an average coefficient of 25:

$$q_{c1Ncs} = 25K_D \tag{12}$$

which is compatible with the approach described by Ref. [8], also used by Ref. [9]. By substituting Eq. (12) into Eq. (8) proposed by Refs. [1,4] obtained the new *CRR*-K_D curve (Fig. 1):

$$CRR = exp\left(0.001109K_D^4 - 0.00569K_D^3 + 0.000625K_D^2 + 0.221K_D - 2.8\right) \tag{13}$$

Differences between Eq. (13) and the most recent previous DMT-based curve proposed by Ref. [9] are observed for K_D lower than 3 and higher than 6 (Fig. 1).

However, like other existing DMT-based methods, the method proposed by Ref. [4] is valid for clean sand and its general application is limited by the lack of a correction factor for the fines content.

3. Proposed methodology

Fig. 3 shows the flowchart of the proposed methodology for the estimation of the *CRR* of the soils from DMT, accounting for the fines content effect. The horizontal stress index, K_D is still the parameter used to evaluate the liquefaction resistance, but it has been modified to account for the fines content effect.

Basically, the approach proposed for DMT follows the approach implemented by Ref. [1] in CPT- and SPT-based methods, in which the *CRR* is estimated as a function of a normalized soil resistance parameter, including the effect of the fines content. Following the above-mentioned approach, in this study the horizontal stress index corrected for the fines content, hereafter called $K_{D,cs}$, is calculated as:

$$K_{D,cs} = K_D + \Delta K_D \tag{14}$$

where K_D is already a normalized parameter and consequently saves its original definition, and ΔK_D is the increment of the horizontal stress index, calculated as a function of the fines content.

While K_D is obtained as an output of the DMT, the increment of the horizontal stress index, ΔK_D needs to be defined as a function of the fines content. The ΔK_D values could be calculated based on *FC* data from laboratory grain size distribution analyses on samples retrieved from nearby boreholes, whenever available. However, in a routine site investigation, this information is rarely available during the execution of the in-situ testing campaign. Therefore, an estimation of the fines content based on the DMT results would be useful, at least for a preliminary evaluation.

For this purpose, the material index I_D obtained by DMT interpretation, defined by Ref. [5] to identify soil type, appears as a suitable parameter. In fact, I_D is a parameter that reflects the mechanical soil behavior, not a soil classification index based on real grain size distribution, similarly to the soil behavior type index I_c obtained from CPT. A relationship between DMT-I_D and CPT-I_c was proposed by Ref. [12], considering the similar intended use of these two parameters. According to this relationship, the value $I_c = 2.6$ generally assumed as an approximate boundary between sand-like and clay-like behavior for CPT corresponds roughly to $I_D \approx 1$ for DMT. This I_D value can be used in DMT-based liquefaction assessment as a threshold value to screen out clay-like soils (having $I_D < 1$), similar to $I_c > 2.6$ in CPT-based methods.

As a consequence, the two output parameters of the DMT to be used in the proposed procedure are: K_D and I_D. The latter can be used to estimate the fines content, then used to quantify the increment of the horizontal stress index for the calculation of the corrected $K_{D,cs}$ (Fig. 3).

Three are the new relationships to be used in comparison with the existing DMT-based methods valid for clean sands only: 1) the estimation of the fines content from the material index, *FC* – I_D relationship; 2) the quantification of the increment of the horizontal stress index due to the fines content, ΔK_D – *FC* relationship; 3) the estimation of the cyclic resistance ratio of the soil for the new upgraded horizontal stress index, *CRR* – $K_{D,cs}$ relationship.

3.1. *FC* – I_D relationships

A correlation *FC* – I_D was recently developed by Ref. [13] for Emilia alluvial plain soils, having the form:

$$FC = x_D(-31I_D + 91) \tag{15}$$

where *FC* is expressed in percentage and x_D is a coefficient ranging from 0.5 to 2.

A large database of experimental data is implicitly incorporated in

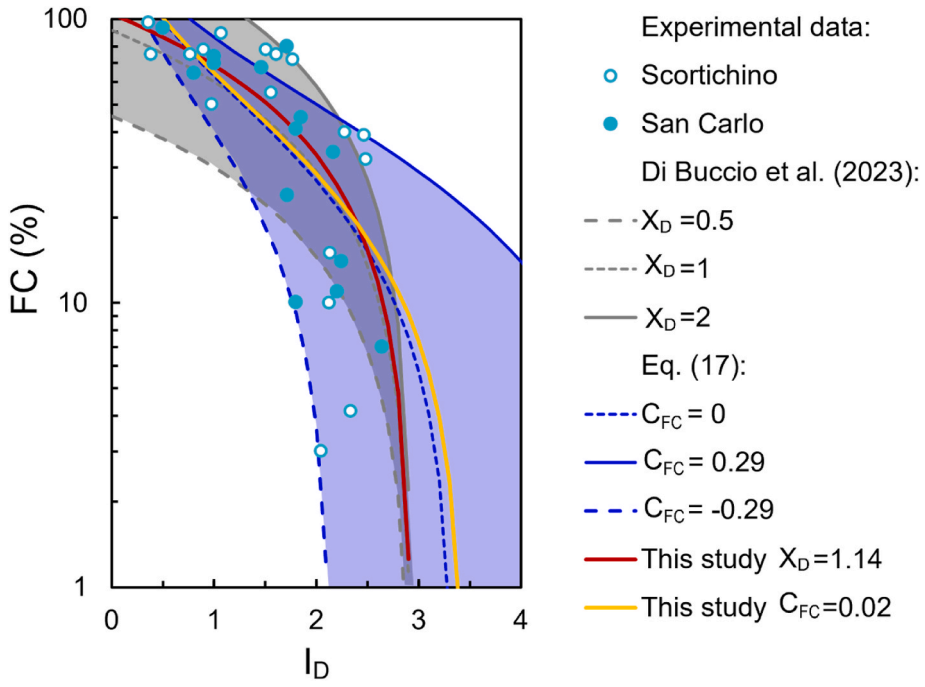

Fig. 4. $FC - I_D$ relationships [13]: and that derived in this study (Eq. (17)) by combining the relationships proposed by Refs. [1,12]. The red and yellow lines represent the calibrated relationships for the considered soils based on the available experimental data. (For interpretation of the references to colour in this figure legend, the reader is referred to the Web version of this article.)

the above relationship.

A different $FC - I_D$ relationship can be obtained considering the link between I_D and I_c reported by Ref. [12]:

$$I_C = 2.5 - 1.5 \log I_D \tag{16}$$

By substituting the expression (16) into equation (7), a general relationship between FC and I_D is obtained as follows:

$$FC = -120 \log I_D + 63 + 80 C_{FC} \tag{17}$$

where C_{FC} is the same correction factor proposed by Ref. [1] to be calibrated on the available data.

A comparison between the two considered relationships is shown in Fig. 4, where experimental $FC - I_D$ data pairs are also reported. Both relationships include the majority of the datapoints, but the [13] relationship is less effective for low values of FC, while Eq. (17) is less effective for high values of FC. Anyway, the mean trends of the two relationships are very close to each other for I_D less than 2.5, approximately. This implies that the two relationships lead to the same FC prediction on average.

Similarly to the I_c versus FC relationship for CPT [1], the large uncertainty in the I_D versus FC relationship for DMT includes contributions from three major factors: (i) Measurement uncertainty that arises from mapping FC values from samples (or some portion of a sample) in a boring to the I_D values (over some interval) from adjacent DMT soundings; heterogeneities in the subsurface, even over short lateral or vertical distances, will contribute to the scatter. (ii) Inherent limitations in using the I_D parameter to predict FC across a broad range of soil types. (iii) Unknown influence of fine plasticity. Distinguishing among these sources of uncertainty is not possible with the currently available information.

Any DMT-based liquefaction triggering evaluation should consider the uncertainty in FC and soil classification estimates when site-specific sampling and lab testing data are not available. In this case, it would be prudent to perform parametric analyses to determine if reasonable variations in the FC and soil classification parameters have a significant effect on liquefaction assessment. Similarly, in DMT-based methods, the cut-off value $I_D \approx 1$ is frequently used to screen out clay-like soils (having $I_D < 1$, corresponding approximately to $I_c > 2.6$ in CPT-based methods), but other values may be justified based on site-specific sampling and testing.

3.2. $\Delta K_D - FC$ relationship

In this study, the same functional form of Eq. (11) is adopted:

$$\Delta K_D = exp\left(a + \frac{b}{FC + c} - \left(\frac{d}{FC + c}\right)^2\right) \tag{18}$$

where a, b, c and d are regression coefficients that need to be calibrated on experimental data.

3.3. $CRR - K_{D,cs}$ relationship

Under the light of this new approach, Eq. (13) can be generalized to all the different types of soils (not only clean sands), as follows:

$$CRR = \exp\left(0.001109 K_{D,cs}^4 - 0.00569 K_{D,cs}^3 + 0.000625 K_{D,cs}^2 + 0.221 K_{D,cs} - 2.8\right) \tag{19}$$

where CRR is the CRR for magnitude 7.5 and an effective confining stress of 1 atm.

3.4. Calibration of the above $\Delta K_D - FC - I_D$ relationships

The proposed approach for incorporating the FC effect in DMT-based liquefaction assessment requires the determination of the regression coefficients a, b, c, d in Eq. (18), as well as x_D or C_{FC} of equations (15) and (17), respectively. At present, these coefficients have not yet been established in a form of general validity, which would require a robust calibration based on large and consistent experimental data sets from different sites. Therefore, the current recommendation is to calibrate the proposed relationships for each specific site by combining relevant data

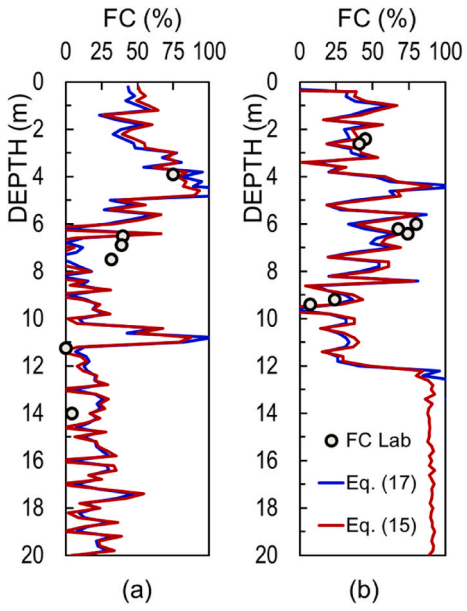

Fig. 5. Comparison of *FC* estimated from I_D, according to Eq. (15) by Di Buccio et al. (2023) and Eq. (17), and *FC* from laboratory tests at the sites of (a) Scortichino, and (b) San Carlo.

from in-situ DMT tests and laboratory tests on samples taken from nearby boreholes. The following procedure is suggested:

1) in the laboratory, obtain *FC* from grain size distribution analyses and *CRR* for magnitude 7.5, corresponding approximately to *CRR* at 15 cycles, from cyclic simple shear or other tests;
2) in situ, obtain I_D and K_D values from DMT at the same depths of the tested samples;
3) calibrate the $FC - I_D$ relationships (Eq. (15) or (17)) based on the *FC* and I_D data pairs;
4) calibrate the proposed $\Delta K_D - FC$ relationship (Eq. (18)) as best-fit of the $CRR\text{-}K_{D,cs}$ correlation (Eq. (19)) based on the same-depth laboratory *FC* and *CRR* and in-situ K_D data.

In this study, the above-mentioned relationships: *FC* as a function of I_D, and ΔK_D as a function of *FC*, are determined in two Italian case studies, where extensive investigation programs were performed after the 2012 Emilia earthquake. The large data set of experimental data obtained by both cyclic laboratory and in-situ tests, including both CPT and DMT, allowed the calibration of the previous $FC - I_D$ and $\Delta K_D - FC$ relationships in a consistent manner.

The first of the two considered case studies is the river dyke of Scortichino, highly damaged by the 2012 Emilia earthquake ([11,14,15]). In one of the investigated cross sections of the dyke one SDMT, one CPTU and one borehole with undisturbed samples of silty sand were performed down to 30 m depth.

The second of the two considered case studies is the village of San Carlo. This inhabited center, part of the municipality of Terre del Reno (Ferrara), was affected by widespread liquefaction in the May 20th, 2012 Emilia earthquake, as documented by several studies ([16–22], among others). The village of San Carlo was constructed above the abandoned channel of the Reno river. The ancient riverbanks can still be recognized as areas morphologically more elevated (about 5–6 m) than the surrounding floodplain. Due to the past river digressions, the sediments in the area are characterized by a complex succession of alluvial deposits belonging to different depositional environments. These deposits consist mostly of sands, silty sands and sandy silts. In the aftermath of the 2012 Emilia earthquake, the area of San Carlo was extensively investigated by a large number of geotechnical and

Table 1
Data used for the calibration of Eq. (18).

Site	Depth (m)	*CRR_field* (15 cycles)	*FC* (%)	K_D	$K_{D,cs}$	ΔK_D
Scortichino	6.4	0.180	39.9	2.1	4.95	2.85
	6.4	0.180	72	1.5	4.95	3.45
San Carlo	6.30	0.139	70.2	1.84	4.06	2.22
	9.25	0.140	12.5	2.50	4.09	1.59
	9.40	0.153	10.4	2.69	4.44	1.75

geophysical in-situ tests carried out by various working groups. The available experimental data set comprises several boreholes, piezocone (CPTU) and seismic piezocone (SCPTU) tests. Four seismic dilatometer tests (SDMT) were carried out in 2013 as part of the INGV-DPC – S2-2012 "COBaS" project [23]. Laboratory tests, including cyclic triaxial tests and resonant column tests, were carried out on undisturbed samples taken from the boreholes.

3.5. Calibration of the $FC - I_D$ relationships

The $FC - I_D$ relationship by Ref. [13] (Eq. (15)) was calibrated based on data pairs of *FC* determined in the laboratory on samples taken from boreholes close to the SDMT soundings and same-depth I_D values from SDMT for both sites (dots in Fig. 4). By combining the data from both sites under study, the application of Eq. (15) provided a value of the coefficient $x_D = 1.14$. The same procedure was applied for the calibration of Eq. (17) by leading to a C_{FC} factor equal to 0.02. The comparison between the two calibrated curves is reported in Fig. 4. The curves are close to each other, with a substantial difference only for $I_D > 2.5$, and also close to the mean trends of the respective relationships. Comparison between the predicted *FC* values obtained along the depth for representative SDMTs performed in the two sites are reported in Fig. 5. The two predicted *FC* profiles do not significantly differ from each other and the performance with respect to the experimental laboratory *FC* values is more or less the same.

3.6. Calibration of the $\Delta K_D - FC$ relationship

The proposed $\Delta K_D - FC$ relationship, described by Eq. (18), was calibrated for these specific sites by assuming as a reference the results of cyclic triaxial tests performed on undisturbed silty sand samples taken from boreholes close to the SDMT soundings in the case of San Carlo, and the results of cyclic simple shear tests performed on undisturbed silty sand samples taken from a borehole close to the SDMT sounding in the case of Scortichino. The undisturbed samples were retrieved from the boreholes in Scortichino with a Shelby tube sampler as reported in Ref. [11], where the undisturbed samples were retrieved using the Osterberg piston sampler in San Carlo site, as reported in Refs. [24,25].

For level ground conditions, earthquake loading is best approximated as two-directional simple shear loading, so the *CRR* from the

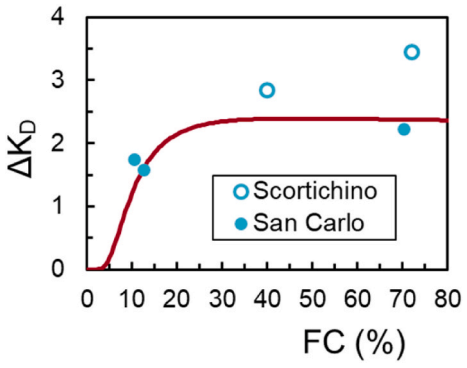

Fig. 6. Calibration of the $\Delta K_D - FC$ relationship for the considered case studies.

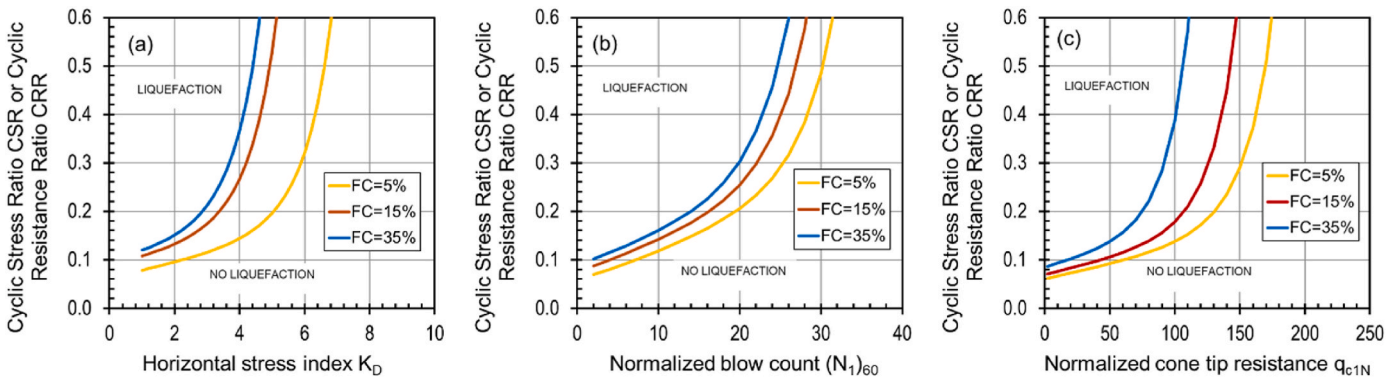

Fig. 7. (a) DMT-based triggering correlation proposed in this study, (b) SPT-based and (c) CPT-based triggering correlation for clean sands and for cohesionless soils having various values of *FC* as proposed by Ref. [1].

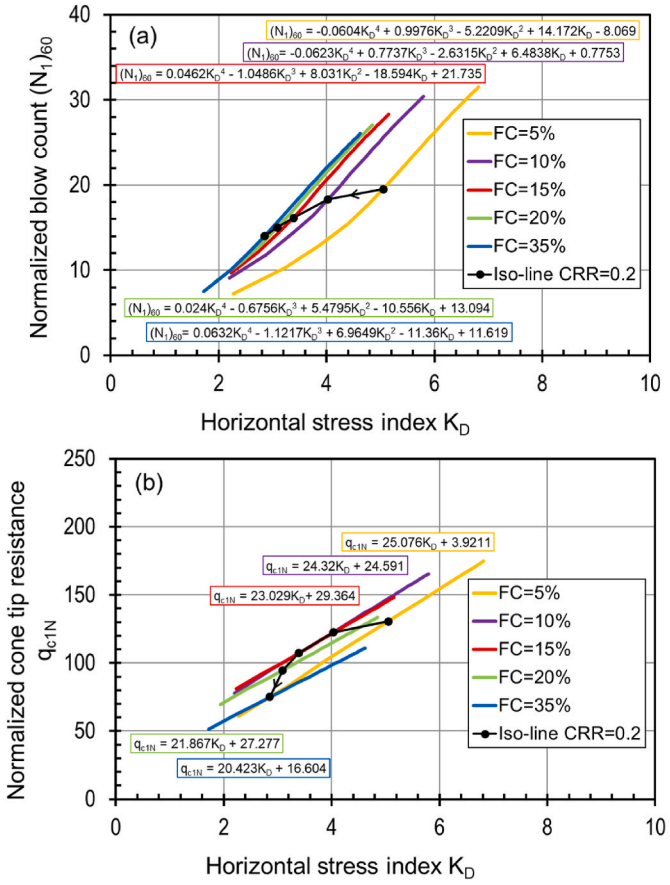

Fig. 8. (a) Relationship between $(N_1)_{60}$ and K_D and (b) between q_{c1N} and K_D.

laboratory tests was reduced by 10 % to represent the in-situ conditions [26]. In addition, the *CRR* from the cyclic triaxial tests has been furtherly reduced by multiplying by a total factor of 0.60 (i.e., the product of 0.9 and 0.67) to account for the differences between the triaxial and the simple shear conditions [26].

For each tested sample, by coupling the *CRR* obtained at 15 cycles (corresponding approximately to *CRR* for magnitude 7.5) and the same-depth K_D from SDMT, the related $K_{D,cs}$ was back-calculated by inverting the relationship in Eq. (19). Then ΔK_D was derived from Eq. (14) and associated to the *FC* for calibration of the *a*, *b*, *c*, *d* coefficients in Eq. (18). To account for the more sophisticated sampling technique adopted in San Carlo compared to Scortichino site, more weight to the data coming from the second case history has been assigned in the calibration process of the coefficients of Eq. (18). The data used for the calibration are reported in Table 1.

The resulting $\Delta K_D - FC$ relationship, shown in Fig. 6, is the following:

$$\Delta K_D = exp\left(0.8 + \frac{7.12}{FC - 2.06} - \left(\frac{13.22}{FC - 2.06}\right)^2\right) \quad (20)$$

Fig. 7 shows the variability of the calibrated *CRR*-K_D relationship, where the comparison with the CPT-based and SPT-based diagrams is also reported. It can be observed that the soil resistance increases as *FC* increases, as expected.

As a further insight, Fig. 8 shows the relationship of K_D against $(N_1)_{60}$ and q_{c1N}. Each pair $(N_1)_{60}$ *vs.* K_D reported in Fig. 8a has been inferred from the *CRR*-$(N_1)_{60}$ and *CRR*-K_D relationships (Fig. 7) by imposing the same *CRR* and *FC* values. Similarly, for the q_{c1N} vs. K_D plot in Fig. 8b. The iso-lines *CRR* = 0.2 are shown in the plots as an example. Following the black arrows on the iso-lines, it is possible to observe that, as the fines content increases, the values of K_D, $(N_1)_{60}$ and q_{c1N} decrease, as expected.

In Fig. 8a and b, the relations of K_D against $(N_1)_{60}$, and q_{c1N}, respectively, have been distinguished for different *FC* values.

As *FC* increases, the $(N_1)_{60}$ *vs.* K_D curves move from left to right (Fig. 8a) because SPT and DMT share the same functional shape to express the beneficial effect of *FC*, i.e., Eq. (11) and Eq. (20), respectively.

As *FC* increases, the angular coefficient of the q_{c1N} - K_D lines decreases (Fig. 8b). The relation between q_{c1N} and K_D differs from that observed between $(N_1)_{60}$ and K_D because, in the CPT-based liquefaction assessment method, the equation that describes the effect of the *FC* (Eq. (6)) is incorporating q_{c1N} in addition to *FC*.

The curves $(N_1)_{60}$ *vs.* K_D are well-described by a fourth-order polynomial function, while the curves q_{c1N} vs. K_D follow a linear trend. All the equations have a coefficient of determination, R^2, equal to 1.

The equations shown in Fig. 8 are not intended as general relationships to be used to convert DMT into CPT or SPT parameters and vice versa, but as the result of mapping the representative parameters for the purpose of liquefaction assessment according to the triggering curves for different *FC* shown in Fig. 7.

3.7. Comparison between the proposed method and that by Chiaradonna and Monaco (2022), not accounting for the fines content effect

Fig. 9 compares the assessment of the soil liquefaction potential by adopting the proposed approach that accounts for the fines content effect and the previous one only for clean sand as proposed by Ref. [4]. The depth profile of *FC* has been estimated through the equation proposed by Ref. [13] calibrated as in the previous section and the corrected $K_{D,cs}$ profile by applying Eqs. (20) and (19).

For the case of Scortichino, the $K_{D,cs}$ significantly differ from the K_D between 1 m and 6 m depth from the ground surface and after 10 m,

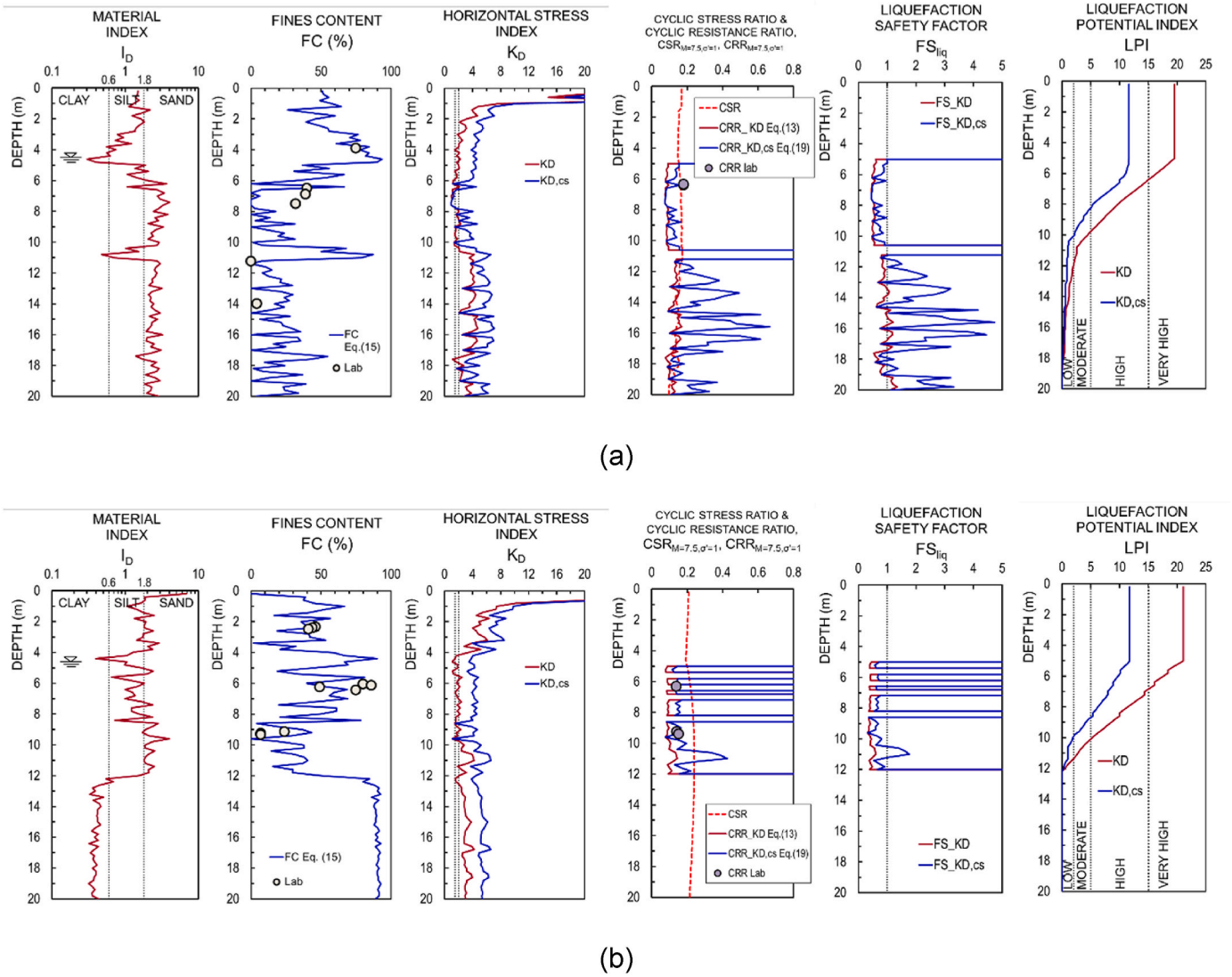

Fig. 9. Assessment of the soil liquefaction potential by adopting the DMT-based method proposed in this study (blue lines) and the method by Ref. [4] (red lines) for the sites of (a) Scortichino and (b) San Carlo. (For interpretation of the references to colour in this figure legend, the reader is referred to the Web version of this article.)

where the lowest values of I_D are measured and the higher fines content is expected, consequently (Fig. 9a). Similar comments can be done for the case of San Carlo, where remarkable differences can be observed along the entire profile (Fig. 9b).

For the liquefaction assessment, the considered seismic scenario is the May 20th, 2012 mainshock, having moment magnitude $M_w = 6.1$. An estimated maximum acceleration $a_{max} = 0.26$ g, equal to the recorded value at the recording station of Mirandola [27], has been adopted at the Scortichino site in the cyclic stress ratio (*CSR*) computations according to the simplified expression reported by Ref. [1]. For the San Carlo site, a maximum acceleration $a_{max} = 0.46$ g has been adopted, equal to the estimated value reported by Ref. [28].

For both DMT-based methods, *CSR* at each depth and the magnitude scaling factor (MSF) were calculated according to Ref. [26]. The groundwater table depth below the ground surface was assumed equal to 4.60 m at San Carlo and 4.50 m at Scortichino, as observed during the site investigations.

The *CRR* estimated by Eq. (19) is generally higher than the *CRR* obtained without the *FC* correction (Eq. (13)), and this leads to a higher safety factor against liquefaction along the soil column.

The "integral" liquefaction susceptibility at the two test locations has been finally evaluated using the liquefaction potential index *LPI* proposed by Ref. [29], according to the modified form proposed by Ref. [30]. The comparison between the two *LPI* plots highlights remarkable differences in the first 12 m and 16 m depth for San Carlo and Scortichino, respectively, and a different classification of the soil liquefaction potential, moving from 'very high' to 'high' or 'moderate' when the effect of the fines content is considered (Fig. 9). On the other hand, the introduction of the *FC* correction does not affect the identification of the main liquefiable layer, which is detected at depths between about 5 m and 12 m at both sites. It is worth noting that the liquefaction manifestations are correctly predicted by the DMT-based methods in both Scortichino and San Carlo sites.

Fig. 10a shows the comparison between predicted and measured *FC* values according to the *FC*-I_D relationships proposed by this study (Eq. (17)) and Di Buccio et al., 2023 (Eq. (15)). On average, both *FC*-I_D relationships overestimate low *FC* values and underestimate high *FC* values. Both provide a good prediction for $FC = 50$ %. Finally, for one of the two cases considered (Scortichino), the Di Buccio et al. (2023) prediction provides negative values of FC.

Fig. 10b compares the measured *CRR* values from the laboratory tests and those predicted by the K_D-based methods by accounting (Eq. (19))

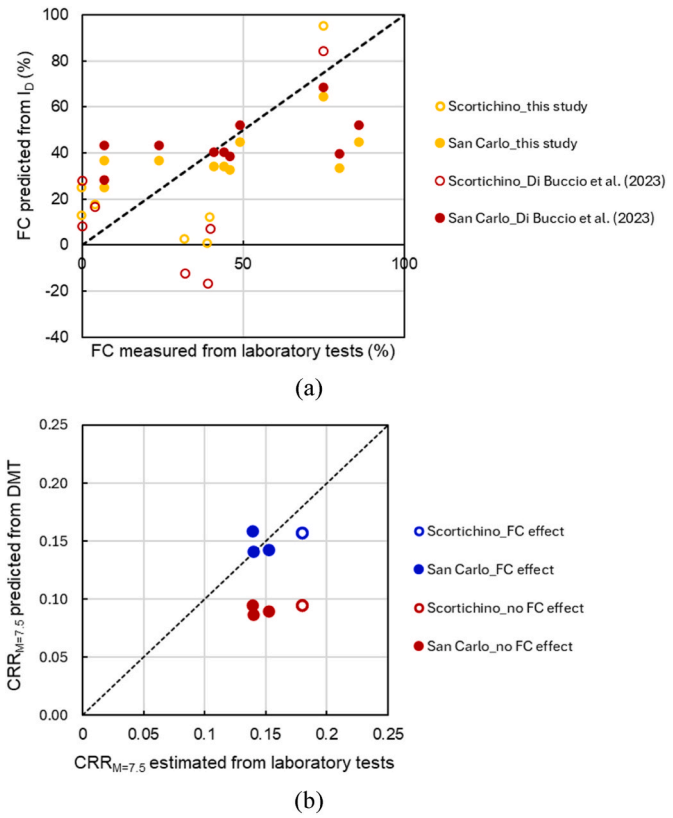

Fig. 10. Validation of the proposed K_D-based method on Scortichino (empty symbols) and San Carlo (full symbols) sites: (a) comparison between predicted and measured *FC* values according to the *FC*-I_D relationships proposed by this study (Eq. (17)) and Di Buccio et al., 2023 (Eq. (15)); (b) comparison between the estimated $CRR_{M=7.5}$ values from the laboratory tests and those predicted by the K_D-based methods accounting for the fines content effect ('FC effect' in legend – blue symbols) according to Eq. (19) or not accounting for the fines content effect ('no FC effect' in legend – red symbols) according to Eq. (13). (For interpretation of the references to colour in this figure legend, the reader is referred to the Web version of this article.)

or not accounting (Eq. (13)) for the fines content effects. It is possible to observe that accounting for the fines content effect allows to for improving significantly the *CRR* prediction, with *CRR* values close to the values evaluated with cyclic laboratory tests. Without the fines content correction, the K_D-based method leads to a significant underestimation of the *CRR* of the soils, reasonable only for clean sands. This implies that, despite the many limitations of the study (limited number of data, rough *FC*-I_D correlation and so on), the application of the proposed method provides undoubtful benefits in the assessment of the *CRR* and of the safety factor against liquefaction.

3.8. Comparison between the proposed DMT-based and the CPT-based methods

Fig. 11 compares the assessment of the soil liquefaction potential by adopting the new DMT-based approach that accounts for the fines content effect and the CPT-based method as proposed by Ref. [1]. The input data were obtained from CPTU soundings carried out close to the SDMT soundings. The results obtained by the DMT-based method by Ref. [4] are also shown in Fig. 11 for comparison.

The two independent approaches lead substantially to the same *LPI* profiles in the case of Scortichino (Fig. 11a), except for the soil layer between about 6 m and 8 m. This difference is due to the fact in this soil deposit, the soil behavior type index I_c is higher than the cut-off value of 2.6, above which the soil is considered non-liquefiable. Conversely, the I_D profile evidences a soil behavior that can be assumed representative of a liquefiable soil. In the case of San Carlo (Fig. 11b) the $LPI \approx 17$ obtained from CPT is an intermediate value between the *LPI* obtained from DMT without and with the *FC* correction (about 21 and 9, respectively). The two approaches identify substantially the same liquefiable layer, except in the depth interval between about 4.6 m and 6.5 m, where some soil layers could have been screened out as "clay-like" based on CPT having $I_c > 2.6$, but not based on DMT having $I_D > 1$. However, the experiments performed in the laboratory showed a clear susceptibility to soil liquefaction of these deposits, and confirmed that the characterization of intermediate soils is a challenging task that requires further studies.

4. Discussion

The approach adopted in this study to account for the effects of fines on DMT-based liquefaction triggering correlations, as a first attempt, is a simple transposition of the approach implemented in CPT- and SPT-based methods by Ref. [1]. Therefore, it is implicitly assumed that the mechanics underlying the need for the fines correction for CPT tip resistance, SPT blow count, and DMT horizontal stress index are similar.

By adopting the penetration and membrane pressurization rates prescribed by the existing standards [31,32], in silty sands, most of the excess pore water pressures around the blade would seemingly be generated during the penetration of the blade rather than during the expansion of the membrane, particularly for the first pressure reading and the derived normalized parameter K_D. In this case, if the time interval between stopping the blade penetration and expanding the membrane was long enough for the excess pore water pressures to dissipate before the membrane is expanded, in principle, there would be no need for a fines correction. This is somewhat implied in Fig. 4, where I_D is constant for a *FC* up to around 10 %. However, for soils with $FC >$ 10 %, the time interval between stopping advancement of the blade and membrane expansion might not be long enough for the excess pore pressures to dissipate and a fines correction is needed.

One option that deserves to be investigated in silty soils could be to increase the time between stopping the blade penetration and expanding the membrane to ensure all the excess pore water pressures generated during the blade penetration have dissipated, thus alleviating the need for a fines correction. The above considerations may provide guidance for future research trends, currently in progress [33–35].

At the present stage, the approach proposed in this study to account for the effects of fines on DMT-based liquefaction triggering correlation has some practical utility, also in consideration of the convenience of setting a short test duration, which largely impacts the professional applications.

5. Conclusions

Simplified methods for liquefaction assessment based on DMT, which make use of the horizontal stress index K_D as an index parameter, may offer a useful addition to current popular methods based on CPT (or SPT, or V_S). This potential is in line with the general recommendation towards the use of "redundant" correlations based on different in-situ techniques/parameters in the "simplified procedure".

This study proposed an upgrade of the existing methods for soil liquefaction assessment based on DMT developed for clean sand, by accounting for the beneficial effects of the fines content on the soil cyclic resistance.

Accounting for the fines content effect allows for improving significantly the prediction of the cyclic soil strength, with values closer to those obtained from cyclic laboratory tests. Without the fines content effect, the K_D-based method leads to a significant underestimation of the cyclic resistance of soils, which is reasonable only for clean sands. This implies that, despite the many limitations of the study (limited number of experimental data, rough *FC*-I_D correlations and so on), the

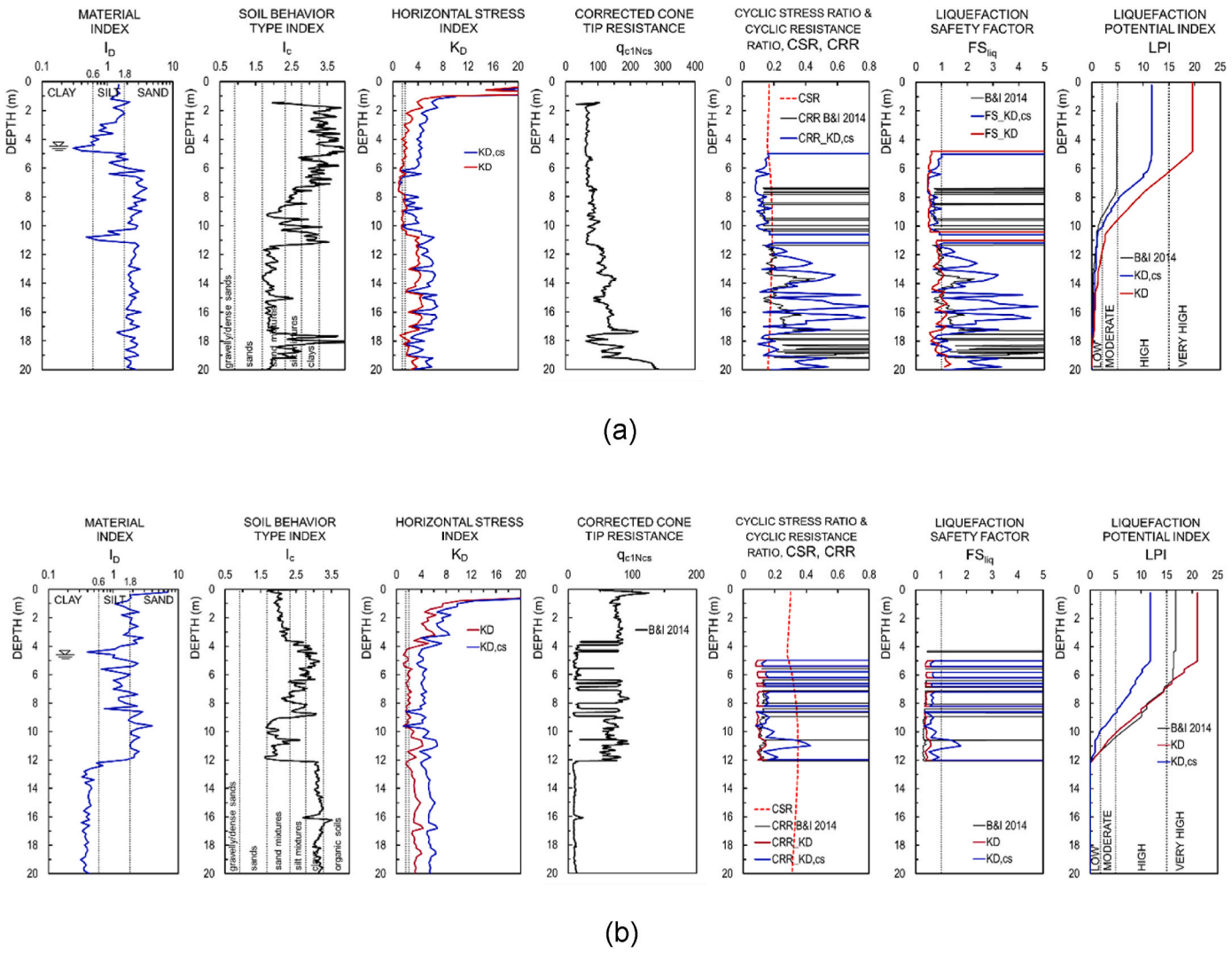

Fig. 11. Assessment of the soil liquefaction potential by adopting the DMT-based method proposed in this study (blue lines), the method by Ref. [4] (red lines) and the CPT-based method by Ref. [1] (black lines) for the sites of (a) Scortichino and (b) San Carlo. (For interpretation of the references to colour in this figure legend, the reader is referred to the Web version of this article.)

application of the proposed method provides undoubtful benefits in the assessment of the safety factor against liquefaction.

In the two examined case studies the new approach allowed the reduction of the discrepancy of the results obtained when the CPT-based method proposed by Ref. [1] is adopted. Some mismatch in the trends provided by the DMT- and CPT-based methods for soils in the silt region, variable from one site to another, could reflect an inaccurate correspondence between the "cut-off" values, used to screen out liquefiable and non-liquefiable soils, of the respective soil behavior type parameters (i.e., I_D and I_c).

The necessary relationships for the implementation of the fines correction have been defined for Italian silty sand/sandy silt deposits affected by liquefaction after the 2012 Emilia earthquake. Future studies are necessary to confirm or disclaim the results obtained in different seismic and soil conditions.

The implementation of an adequate case history database for validation of the DMT-based approach, taking into account the fines content influence, could help address the challenging task of characterizing the liquefaction behavior of intermediate soils.

CRediT authorship contribution statement

Anna Chiaradonna: Writing – review & editing, Writing – original draft, Visualization, Validation, Methodology, Formal analysis, Data curation, Conceptualization. **Paola Monaco:** Writing – review & editing, Writing – original draft, Visualization, Validation, Supervision, Resources, Project administration, Methodology, Investigation, Funding acquisition, Data curation.

Declaration of competing interest

The authors declare that they have no known competing financial interests or personal relationships that could have appeared to influence the work reported in this paper.

Acknowledgements

This work has been supported by the Research Project of National Interest 'TRANSITION – characTeRization And modelling of iNtermediate Soils through Innovative approaches for robust design of straTegic Infrastructures and protection Of risk-seNsitive areas' funded by the Italian Ministry of University and Research (PRIN 2022 – Project 2022PZW7FL – Grant E53D23003630006) and by the Research Project ReLUIS-DPC 2024–2026 (WP16 – Task 1 'Site seismic stability') funded by the Italian Civil Protection Department.

The experimental data at the Scortichino site presented in this paper

were obtained as part of the activity of the AGI-RER Working Group, promoted by the Emilia-Romagna Regional Authority (RER) in cooperation with the Italian Geotechnical Society (AGI).

The SDMT tests at the San Carlo site were carried out as part of the Project INGV-DPC 2012–2013 – S2-2012 'COBaS: Constraining Observations into Seismic Hazard' (Task 8 'Liquefaction' coordinated by Prof. Roberto W. Romeo). Additional information and data from in-situ and laboratory tests at the site were shared within the scope of the same project.

The authors are grateful to Dr Luca Martelli and the Geological, Seismic and Soil Survey of the Emilia-Romagna Regional Authority (RER) for providing access to the RER soil investigation database.

Additionally, the authors would like to thank Romualdo Cecchi for his valuable contribution during the Master Thesis in Civil Engineering at the University of L'Aquila.

Finally, the authors would like to thank Prof. Russel Green and the anonymous reviewers for their insightful comments, which have much enhanced the quality of the study.

Data availability

Data will be made available on request.

References

[1] Boulanger RW, Idriss IM. CPT and SPT liquefaction triggering procedures. Davis, USA: University of California at; 2014. Report No. UCD/GCM-14/01.
[2] Chiaradonna A, Monaco P. Estimation of the soil cyclic resistance by flat dilatometer accounting for the fines content effect. Proc 8th Int Conf Earthquake Geotech Eng 8ICEGE 2024;10(27):1013–8. https://doi.org/10.3208/jgssp.v10.OS-16-06. Osaka, Japan, Japanese Geotechnical Society Special Publication.
[3] Cecchi R, Chiaradonna A, Monaco P. DMT-based liquefaction assessment accounting for the fines content effect: a case study in Emilia-Romagna, Italy. Proc 7th Int Conf Geotech Geophy Site Characteriz 2024:1533–9. https://doi.org/10.23967/isc.2024.142. Barcelona, Spain.
[4] Chiaradonna A, Monaco P. Assessment of liquefaction triggering by seismic dilatometer tests: comparison between semi-empirical approaches and non-linear dynamic analyses. Proc 20th Int Conf Soil Mech Geotech Eng ICSMGE 2022;2:335–40. 2022, Sydney, Australia.
[5] Marchetti S. In situ tests by flat dilatometer. J Geotech Eng Div 1980;106(GT3):299–321.
[6] Monaco P, Marchetti S, Totani G, Calabrese M. Sand liquefiability assessment by flat dilatometer test (DMT). Proc 16th Int Conf Soil Mech Geotech Eng 2005;4:2693–7. https://doi.org/10.3233/978-1-61499-656-9-2693. Osaka, Japan.
[7] Tsai P, Lee D, Kung GT, Juang CH. Simplified DMT-based methods for evaluating liquefaction resistance of soils. Eng Geol 2009;103:13–22. https://doi.org/10.1016/j.enggeo.2008.07.008.
[8] Robertson PK. The James K. Mitchell Lecture: interpretation of in-situ tests – some insights. Proc 4th Int Conf Geotech Geophy Site Characteriz ISC'4, Porto de Galinhas 2012;1:3–24. Brazil.
[9] Marchetti S. Incorporating the stress history parameter K_D of DMT into the liquefaction correlations in clean uncemented sands. J Geotech Geoenviron Eng 2016;142(2):04015072. https://doi.org/10.1061/(ASCE)GT.1943-5606.0001380.
[10] Monaco P. Combined use of CPT & DMT: background, current trends and ongoing developments, Cone Penetration Testing 2022. Proc 5th Int Sympos Cone Penetration Testing CPT'22 2022:94–106. https://doi.org/10.1201/9781003308829-7. Bologna, Italy.
[11] Tonni L, Gottardi G, Amoroso S, Bardotti R, Bonzi L, Chiaradonna A, d'Onofrio A, Fioravante V, Ghinelli A, Giretti D, Lanzo G, Madiai C, Marchi M, Martelli L, Monaco P, Porcino D, Razzano R, Rosselli S, Severi P, Silvestri F, Simeoni L, Vannucchi G, Aversa S. Interpreting the deformation phenomena triggered by the 2012 Emilia seismic sequence on the Canale Diversivo di Burana banks. Riv Ital Geotec 2015;49(2):28–58 (in Italian).
[12] Robertson PK. CPT-DMT correlations. J Geotech Geoenviron Eng 2009;135(11):1762–71. https://doi.org/10.1061/(ASCE)GT.1943-5606.0000119.
[13] Di Buccio F, Comina C, Fontana D, Minarelli L, Vagnon F, Amoroso S. Fines content determination through geotechnical and geophysical tests for liquefaction assessment in the Emilia alluvial plain (Ferrara, Italy). Soil Dynam Earthq Eng 2023;173:108057. https://doi.org/10.1016/j.soildyn.2023.108057.
[14] Chiaradonna A, Tropeano G, d'Onofrio A, Silvestri F. Interpreting the deformation phenomena of a levee damaged during the 2012 Emilia earthquake. Soil Dynam Earthq Eng 2019;124:389–98. https://doi.org/10.1016/j.soildyn.2018.04.039.
[15] Chiaradonna A, Monaco P, Tropeano G. Variability of the seismic response of a liquefiable soil with the fines content as estimated via dilatometer tests. Proc 7th Int Conf Geotech Geophy Site Characteriz 2024. https://doi.org/10.23967/isc.2024.232. Barcelona, Spain.
[16] Vannucchi G, Crespellani T, Facciorusso J, Ghinelli A, Madiai C, Puliti A, Renzi S. Soil liquefaction phenomena observed in recent seismic events in Emilia-Romagna Region (Italy). Ingegneria Sismica 2012;29(2–3):20–30.
[17] Emergeo Working Group. Liquefaction phenomena associated with the Emilia earthquake sequence of May–June 2012 (Northern Italy). Nat Hazards Earth Syst Sci 2013;13(4):935–47. https://doi.org/10.5194/nhess-13-935-2013.
[18] Fioravante V, Giretti D, Abate G, Aversa S, Boldini D, Capilleri PP, Cavallaro A, Chamlagain D, Crespellani T, Dezi F, Facciorusso J, Ghinelli A, Grasso S, Lanzo G, Madiai C, Massimino MR, Maugeri M, Pagliaroli A, Rainieri C, Tropeano G, Santucci De Magistris F, Sica S, Silvestri F, Vannucchi G. Earthquake geotechnical engineering aspects of the 2012 Emilia-Romagna earthquake (Italy). Proc 7th Int Conf Case Histories Geotech Eng 2013. Chicago, USA, Paper No. EQ-5.
[19] Facciorusso J, Madiai C, Vannucchi G. Soil liquefaction analyses in a test-area affected by the 2012 Emilia-Romagna earthquake (Italy). In: Lollino G, et al., editors. Engineering geology for society and territory, vol 5; 2014. p. 1111–4. https://doi.org/10.1007/978-3-319-09048-1_211.
[20] Facciorusso J, Madiai C, Vannucchi G. CPT-based liquefaction case history from the 2012 Emilia earthquake in Italy. J Geotech Geoenviron Eng 2015;141(12):1032–51. https://doi.org/10.1061/(ASCE)GT.1943-5606.0001349.
[21] Lai CG, Bozzoni F, Mangriotis M-D, Martinelli M. Soil liquefaction during the 20 May 2012 M5.9 Emilia earthquake, Northern Italy: field reconnaissance and post-event assessment. Earthq Spectra 2015;31(4):2351–73. https://doi.org/10.1193/011313EQS002M.
[22] Papathanassiou G, Mantovani A, Tarabusi G, Rapti D, Caputo R. Assessment of liquefaction potential for two liquefaction prone areas considering the May 20, 2012 Emilia (Italy) earthquake. Eng Geol 2015;189:1–16. https://doi.org/10.1016/j.enggeo.2015.02.002.
[23] Romeo RW, Amoroso S, Facciorusso J, Lenti L, Madiai C, Martino S, Monaco P, Rinaldis D, Totani F. Soil liquefaction during the Emilia, 2012 seismic sequence: investigation and analysis. In: Lollino G, et al., editors. Engineering geology for society and territory, vol 5; 2015. p. 1107–10. https://doi.org/10.1007/978-3-319-09048-1_210.
[24] Romeo RW, Martino S, Monaco P, Totani F, Madiai C, Facciorusso J, Rinaldis D, Lenti L. D. 8.1 – report on liquefaction phenomena and shaking causative levels. Deliverable of the DPC-INGV-S2 project "constraining observations into Seismic hazard. 2013.
[25] Santisi d'Avila MP, Lenti L, Martino S, Romeo RW. Nonlinear numerical simulation of the soil seismic response to the 2012 Mw 5.9 emilia earthquake considering the variability of the water table position. Bull Seismol Soc Am 2013;109(2):505–24. https://doi.org/10.1785/0120170345.
[26] Idriss IM, Boulanger RW. Soil liquefaction during earthquakes, EERI publication No. MNO-12. Oakland, USA: Earthquake Engineering Research Institute; 2008.
[27] D'Amico M, Felicetta C, Russo E, Sgobba S, Lanzano G, Pacor F, Luzi L. Italian accelerometric archive v 3.1. Istituto Nazionale di Geofisica e Vulcanologia; 2020. https://doi.org/10.13127/itaca.3.1. Dipartimento della Protezione Civile Nazionale.
[28] Minarelli L, Amoroso S, Civico R, De Martini PM, Lugli S, Martelli L, Molisso F, Rollins KM, Salocchi A, Stefani M, Cultrera G, Milana G, Fontana D. Liquefied sites of the 2012 Emilia earthquake: a comprehensive database of the geological and geotechnical features (Quaternary alluvial Po plain, Italy). Bull Earthq Eng 2022;20:3659–97. https://doi.org/10.1007/s10518-022-01338-7.
[29] Iwasaki T, Arakawa T, Tokida K. Simplified procedures for assessing soil liquefaction during earthquakes. Int J Soil Dynam Earthq Eng 1984;3(1):49–58. https://doi.org/10.1016/0261-7277(84)90027-5.
[30] Sonmez H. Modification of the liquefaction potential index and liquefaction susceptibility mapping for a liquefaction-prone area (Inegol, Turkey). Environ Geol 2003;44:862–71. https://doi.org/10.1007/s00254-003-0831-0.
[31] ASTM D6635-15. Standard test method for performing the flat plate dilatometer. West Conshohocken, PA, USA: ASTM International; 2015.
[32] ISO 22476-11:2017(E). Geotechnical investigation and testing – field testing – part 11: flat dilatometer test. Geneva, Switzerland: International Organization for Standardization; 2017.
[33] Monaco P, Amoroso S, Chiaradonna A, Marchetti D, Le TMH, L'Heureux J-S. Characterization of intermediate soils by innovative in-situ testing procedures using Medusa DMT. Proc 18th Eur Conf Soil Mech Geotech Eng ECSMGE 2024 2024:679–82. https://doi.org/10.1201/9781003431749-109. Lisbon, Portugal.
[34] Monaco P, Chiaradonna A, Marchetti D, Amoroso S, L'Heureux J-S, Le TMH. The JELLYFISh project: Medusa SDMT testing at the NGTS Geo-Test sites, Norway. Proc 7th Int Conf Geotech Geophy Site Characteris ISC'7 2024:1589–96. https://doi.org/10.23967/isc.2024.205. Barcelona, Spain.
[35] Monaco P, Tonni L, Amoroso S, Garcia Martinez MF, Gottardi G, Marchetti D, Minarelli L. Use of Medusa DMT in alluvial silty sediments of the Po river valley. Proc 6th Int Conf Geotech Geophy Site Characteris ISC'6 2021. https://doi.org/10.53243/ISC2020-424. Budapest, Hungary.